SYNTHESIS AND CHARACTERIZATION OF PYROCHLORE TO ENHANCE THE CHEMICAL AND RADIATION STABILITY OF ACTINIDE-RICH WASTES

S. C. Chae, Y. N. Jang, I. K. Bae
Korea Institute of Geoscience and Mineral Resources
30 Gajeong-dong, Yuseong-gu, Daejeon, 305-350, Korea

S.V. Yudintsev
Institute of Geology of Ore Deposits, Petrography, Mineralogy and Geochemistry
Staromonetny 35, Moscow 119017, Russia

ABSTRACT

Pyrochlore was known to be one of the most promising matrices for the immobilization of actinide-rich high level waste. Especially, its chemical and radiation stability increases strongly by substituting Ti by Zr and probably Hf. This study was aimed at the synthesis, phase relation and characterization of the pyrochlore ($CaCeHf_xTi_{2-x}O_7$, x = 0.2-2.0) produced in the system of Ca-Ce-Hf-Ti-O. Using the Cold pressing and sintering (CPS) method, the mixture of $CaCO_3$, CeO_2, HfO_2 and TiO_2 oxides was pressed, and sintered in the range of 1200°C-1600°C for 20 hr. In all ceramics fabricated pyrochlore coexisted with minor perovskite, or CeO_2. The d-spacings values and unit cell parameters of pyrochlore and perovskite increased with increasing hafnium content. It was suggested that the cell dimension is related to the ionic radii of elements, which occupy not only eight-coordinated site, but also six-coordinated site. Although the ionic radii ratio (r_A^{VIII}/r_B^{VI}=1.45) at x=2.0 was below the stability range of pyrochlore structure, XRD data showed the existence of pyrochlore. We inferred that such discrepancy may be due to the gap of the stability range of pyrochlore structure that was not treated in previous studies or to the difference of the elements occupied the six-coordinated sites.

INTRODUCTION

Immobilization of fissile Pu generated in the nuclear fuel cycle or recovered from dismantled nuclear weapons has become an important issue for the safety and health of mankind. Current strategies generally practiced around the world include immobilizing the Pu in a stable host matrix followed either burning in a nuclear reactor or placing in a geologic repository for ultimate disposal [1]. Vitrification has been studied for a long time as an immobilization method

for the radioactive waste. However, glass is thermodynamically unstable and subjected to devitrificate. It can result in the decrease of its chemical durability and the escape of radionuclides in the environment.

To minimize these disadvantages, Ringwood [2] and Ringwood et al. [3] suggested "Synroc" as an alternative matrix of glass. Their suggestion based on the fact that some natural minerals containing radioactive elements have retained their structure stable for more than millions years. Thereafter, the synthesis and characterization study on various kinds of matrices has been carried out [4-11].

Important parameters for such immobilization matrices are chemical and radiation resistance, and technological effectiveness (efficiency of industrial-scale production) [12].

The CPS method used in this study is one of the common methods applied for matrix synthesis. It is an economic method that requires simple and cheaper equipment than other methods of crystalline matrix production such as hot pressing [11].

Of these confinement materials, pyrochlore was proposed as promising materials for the immobilization of actinide-rich wastes. The pyrochlores typically exhibit $[A_2]^{VIII}[B_2]^{VI}O_7$ stoichiometry, where actinides and lanthanides are incorporated into the A-site, and either Ti, Hf, Sn or Zr occupies the B-site. It has a fluorite-derived structure (space group: Fd3m) where one eighth of oxygen is missing. Two different structural sites for cations (A- and B-sites) exist, resulting in the cell parameter of pyrochlore, which is twice that of the fluorite lattice.

It is known that substitution of Ti with Zr (or probably Hf) in the pyrochlore structure strongly increases chemical and radiation stability of this actinide waste form [13]. Besides Hf, Gd may serve as neutron absorber preventing nuclear chain reaction. Therefore, we intended to synthesize pyrochlore as a target phase, and to characterize the phase relation in the Ca-Ce-Hf-Ti-O system.

Experimental

For synthesis of pyrochlore, $CaCO_3$ (High Purity Chemicals, 4N), TiO_2 (Rare Metallic Co., Ltd., 3N) CeO_2 (Johnson Mattey, 3N), and HfO_2 (Alddrich Co., 98%) were used as starting materials. These powders mixed in the appropriate ratios, corresponding to general formula ($[CaCe][Hf_xTi_{2-x}]O_7$: x = 0.2, 0.6, 1.0, 1.4, 1.8) with alcohol, using an alumina mortar and pestle. The mixed powders were pressed into pellets (10-mm diameter x 2-mm height) at a pressure of 400 kg/cm^2. The pellets were sintered at 1200^{o}C-1600^{o}C for 20 hr. Synthesis was performed in the oxygen atmosphere to maintain Ce in the highest oxidation state (IV). Phase identification was determined by X-ray diffraction (reflection mode, CuKa radiation) using a Phillips X'pert

MPD X-ray diffractometer attached with a graphite monochrometer. The compositions of synthetic phases were analyzed with a SEM/EDS analyzer.

XRD Results

$CaCeHf_xTi_{2-x}O_7$ in case of x=0.2: At 1200°C, pyrochlore already showed the strongest diffraction intensity, and CeO_2 with minor TiO_2 and HfO_2 was also found. Pyrochlore showed the strongest intensity continuously until at 1500°C, and the disappearance of TiO_2 and HfO_2, and abrupt decrease of CeO_2 were observed at 1300°C. At 1400°C, perovskite first formed and increased with increasing temperature (it may be connected with partial reducing Ce into Ce(III) state). Recently published results on the examination of calcium cerium titanate ceramics using X-ray photoelectron spectroscopy method [14] have confirmed this suggestion. From these results, it was confirmed that optimum synthetic condition of pyrochlore was achieved at a temperature of 1300°C. The sample melted completely at 1600°C (Fig. 1a and Table I).

$CaCeHf_xTi_{2-x}O_7$ in case of x=0.6: At 1200°C, CeO_2 showed the strongest diffraction intensity and coexisted with TiO_2, HfO_2, perovskite and pyrochlore. Among starting materials, CeO_2 was observed in all range of temperature but TiO_2 and HfO_2 disappeared at 1300°C and 1400°C, respectively. Perovskite decreased with temperature, and pyrochlore first showed the strongest diffraction intensity at 1400°C. The sample melted at 1600°C as like as one with previous composition at x=0.2 (Fig. 1b and Table I).

$CaCeHf_xTi_{2-x}O_7$ in case of x=1.0: HfO_2, CeO_2 and perovskite coexisted with minor pyrochlore at 1200°C. Among starting materials, HfO_2 first disappeared at 1400°C but CeO_2 showed the strongest diffraction intensity up to 1300°C and abruptly decreased with increasing temperature. Pyrochlore showed the strongest diffraction intensity at 1400°C. Perovskite and pyrochlore showed the contradictory trend to decrease and to increase with increasing temperature, respectively. The sample melted at 1600°C as like as those with two chemical compositions mentioned above (Fig. 1c and Table I).

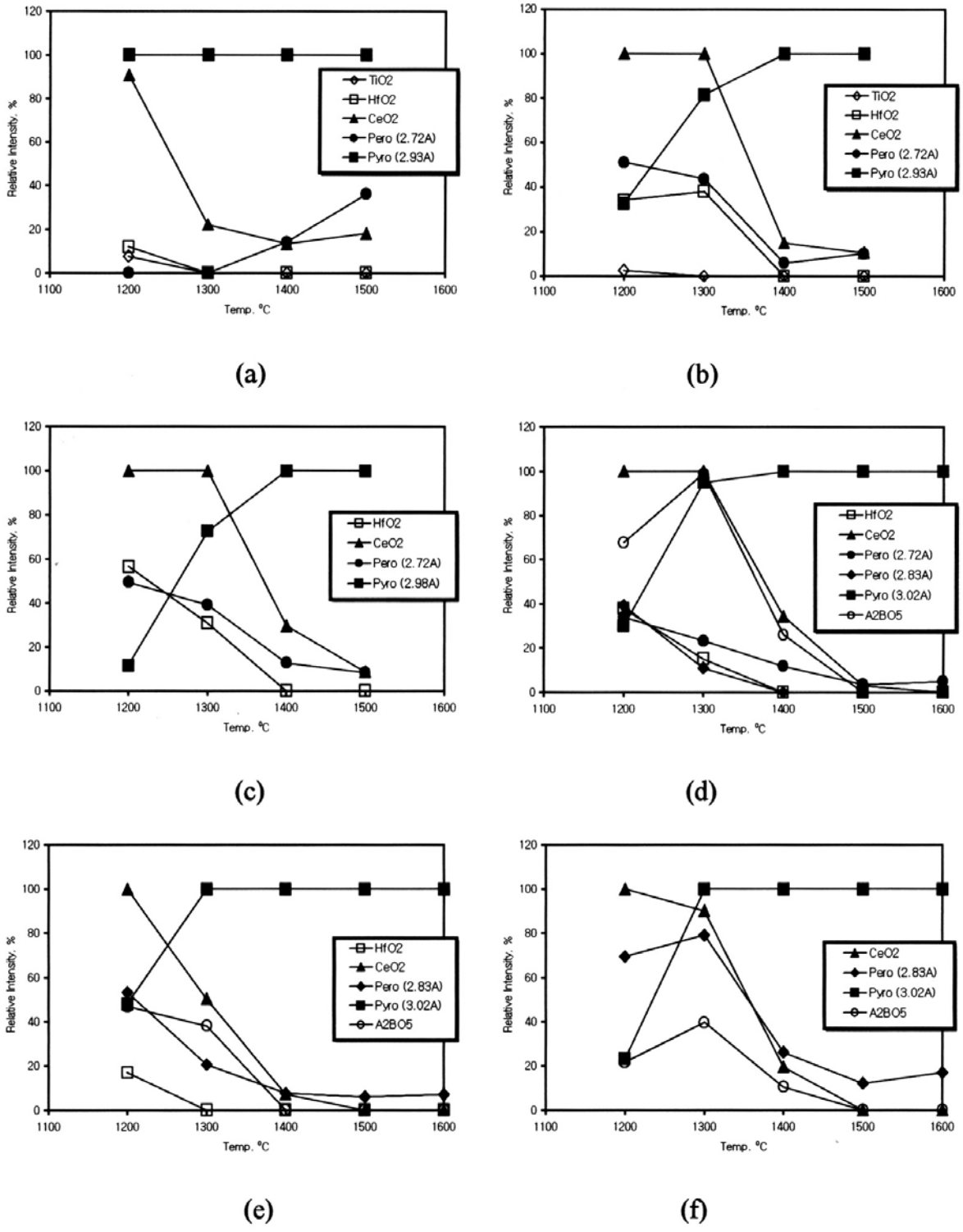

Fig. 1. Relative intensities of phases in the matrices synthesized from the composition of $CaCeHf_xTi_{2-x}O_7$ at (a) x=0.2, (b) x=0.6, (c) x=1.0, (d) x=1.4, (e) x=1.8 and (f) x=2.0. Samples, which were synthesized from the composition at x=0.2-1.0, were melted.

Table I. Relative Intensities of Phases Formed from Various Compositions ($CaCeHf_xTi_{2-x}O_7$: x=0.2-2.0).

Compositions	Temp.	TiO_2 (3.25A)	HfO_2 (3.15A)	CeO_2 (3.13A)	Pero (2.72A)	Pero (2.83A)	Pyro (2.93A)	Pyro (2.98A)	Pyro (3.02A)	A_2BO5 (2.97A)
X=0.2	1200	8	12	91	0	0	100	0	0	0
	1300	0	0	22	0	0	100	0	0	0
	1400	0	0	13	14	0	100	0	0	0
	1500	0	0	18	36	0	100	0	0	0
	1600	Melt								
X=0.6	1200	3	34	100	51	0	33	0	0	0
	1300	0	38	100	44	0	82	0	0	0
	1400	0	0	15	6	0	100	0	0	0
	1500	0	0	11	10	0	100	0	0	0
	1600	Melt								
X=1.0	1200	0	56	100	49	0	0	12	0	0
	1300	0	31	100	39	0	0	73	0	0
	1400	0	0	29	13	0	0	100	0	0
	1500	0	0	9	8	0	0	100	0	0
	1600	Melt								
X=1.4	1200	0	38	100	34	39	0	0	30	68
	1300	0	15	100	23	11	0	0	95	99
	1400	0	0	34	12	0	0	0	100	26
	1500	0	0	3	4	0	0	0	100	0
	1600	0	0	0	5	0	0	0	100	0
X=1.8	1200	0	17	100	0	53	0	0	48	47
	1300	0	0	50	0	21	0	0	100	38
	1400	0	0	7	0	8	0	0	100	0
	1500	0	0	0	0	6	0	0	100	0
	1600	0	0	0	0	7	0	0	100	0
X=2.0	1200	0	0	100	0	70	0	0	23	22
	1300	0	0	90	0	79	0	0	100	40
	1400	0	0	20	0	26	0	0	100	10
	1500	0	0	0	0	12	0	0	100	0
	1600	0	0	0	0	17	0	0	100	0

Pero: Perovskite; Pyro: Pyrochlore
Figures in parenthesis indicates main peak of identified phase in angstrom (A).

$CaCeHf_xTi_{2-x}O_7$ in case of x=1.4: At 1200°C, CeO_2 revealed the strongest diffraction intensity and coexisted with HfO_2, two kinds of perovskites (d=2.72A and d=2.83A), pyrochlore and A_2BO_5 type oxides. Among starting materials, HfO_2 disappeared at 1400°C, and CeO_2 was observed the strongest diffraction intensity up to 1300°C but decreased with increasing temperature and disappeared at 1600°C. With the increase of temperature, the intensity of two kinds of perovskites decreased and perovskite, which have d=2.83A, disappeared at 1300°C. A_2BO_5 oxides showed considerable intensity similar to pyrochlore at 1300°C, but it decreased with increasing temperature and disappeared at 1500°C. Pyrochlore first showed the strongest intensity at 1400°C, and coexisted with minor perovskite at 1600°C (Fig. 1d and Table I).

$CaCeHf_xTi_{2-x}O_7$ in case of x=1.8: At 1200°C, CeO_2 showed the strongest diffraction intensity and coexisted with HfO_2, perovskite, pyrochlore and A_2BO_5 oxides. With the increase of temperature, the intensities of HfO_2, A_2BO_5 oxide, CeO_2 and perovskite gradually decreased, and three phases except perovskite disappeared at 1300°C, at 1400°C and at 1500°C, respectively. Pyrochlore first showed the strongest diffraction intensity at 1300°C and coexisted with minor perovskite in the range of 1500°C-1600°C. That their intensity was not changed from 1500°C to 1600°C indicated that equilibrium state was achieved at 1500°C (Fig. 1e and Table I).

$CaCeHf_xTi_{2-x}O_7$ in case of x=2.0: CeO_2 showed the strongest intensity, and coexisted with perovskite, pyrochlore and A_2BO_5 oxides at 1200°C. CeO_2 and A_2BO_5 oxides disappeared at 1500°C. Pyrochlore first showed the strongest diffraction intensity at 1300°C and coexisted with minor perovskite in the range of 1500°C-1600°C. That their intensity was not changed from 1500°C to 1600°C indicated that equilibrium state was attained at 1500°C as like as at x=1.8 (Fig. 1f and Table I).

SEM/EDS Analysis

Chemical compositions of samples (Fig. 2), which were synthesized in the optimum conditions, were analyzed with a SEM/EDS analyzer. In sample sintered at x=0.2, major pyrochlore coexisted with minor perovskite and HfO_2 (Fig. 3a). In sample sintered at x=0.6, the existence of HfO_2 instead of CeO_2 differed from the data of XRD was found (Fig. 3b). In the range of x between 1.0 and 2.0 (Fig. 3c-e), pyrochlore was the major phase, and minor perovskite were observed too. The compositions of pyrochlore analyzed by EDS were as follows: $[Ca_{0.9}Ce_{0.9-1.0}][Hf_{0.2}Ti_{1.9}]O_7$ at x=0.2, $[Ca_{0.8-0.9}Ce_{0.9-1.0}][Hf_{0.7-0.9}Ti_{1.3-1.4}]O_7$ at x=0.6, $[Ca_{0.8}Ce_{1.0}][Hf_{1.3}Ti_{0.8}]O_7$ at x=1.0, $[Ca_{0.7}Ce_{1.1}][Hf_{1.7}Ti_{0.4}]O_7$ at x=1.4, $[Ca_{0.7-0.8}Ce_{1.1-1.2}][Hf_{1.7-1.9}Ti_{0.2}]O_7$ at x=1.8 and $[Ca_{0.6-0.7}Ce_{1.1}][Hf_{2.1}]O_7$ at x=2.0. Fig. 4 represented the relationship of real chemical and stoichiometric compositions of synthetic pyrochlores. The contents of Ca were less than stoichiometric compositions but those of Ce were more than stoichiometric compositions except for compositional range with "x" between 0.2 and 0.6. Also, the content of Hf was higher than stoichiometric composition in the range of "x" between 0.6 and 1.4, but content of Ti was less than stoichiometric compositions in the range of "x" between 0.6 and 1.0.

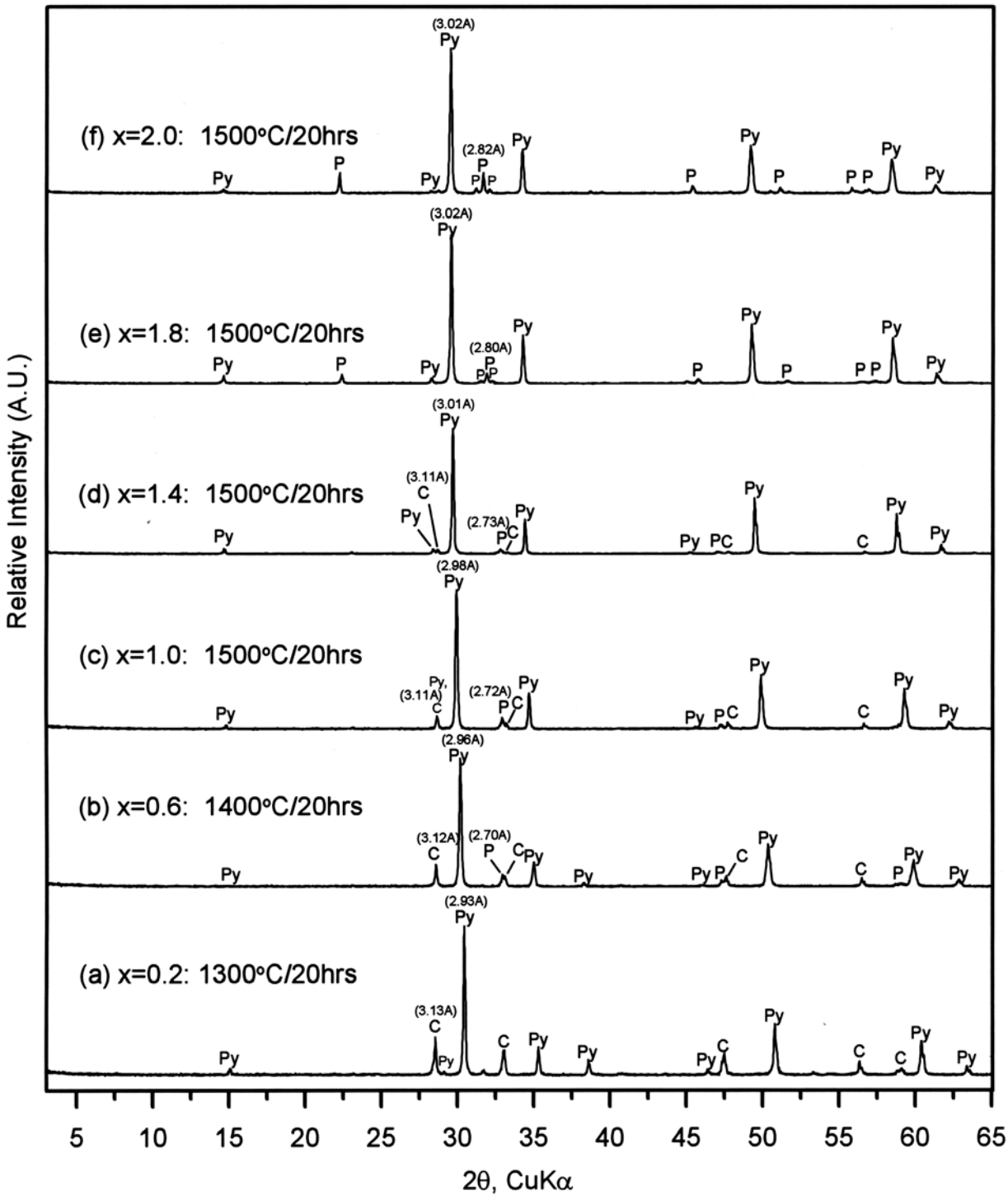

Fig. 2. XRD patterns of phases synthesized in optimum conditions from $CaCeHf_xTi_{2-x}O_7$ batch composition. Abbreviation: Py (Pyrochlore), P (Perovskite), C (CeO_2; Cerianite). Figures in parenthesis indicates the d values of main peaks of identified phases in angstrom (A).

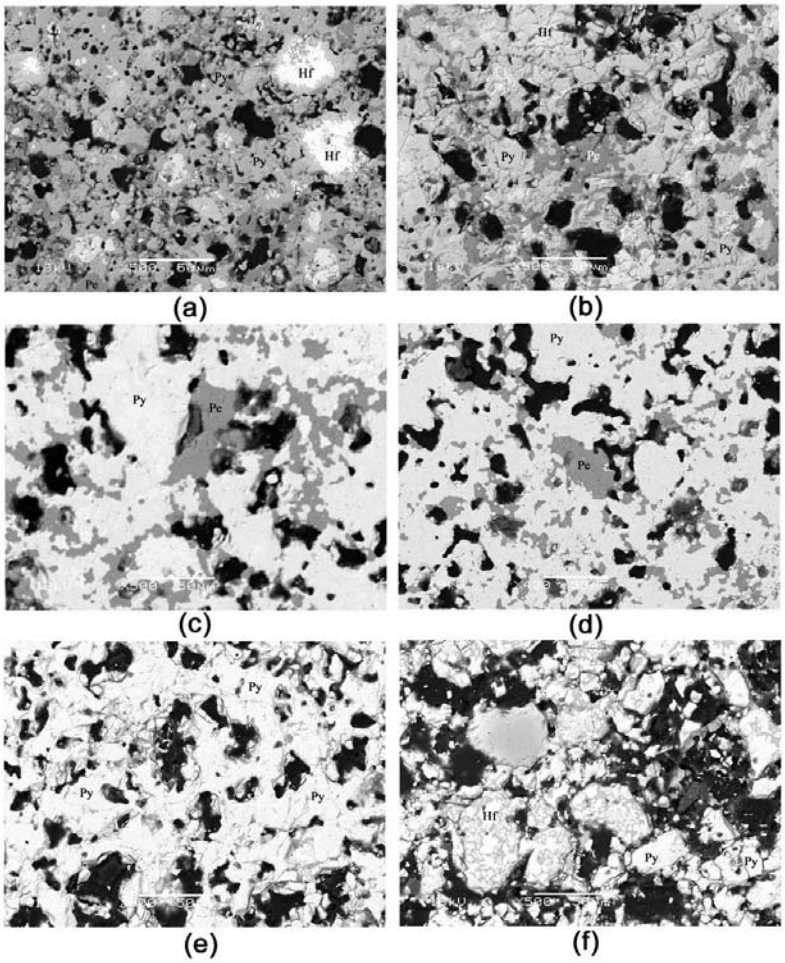

Fig. 3. Back scattering electron images of the samples synthesized from the composition of $CaCeHf_xTi_{2-x}O_7$ at (a) x=0.2, (b) x=0.6, (c) x=1.0, (d) x=1.4, (e) x=1.8 and (f) x=2.0. Abbreviations: Hf (HfO_2); Py (Pyrochlore); Pe (Perovskite). Scale bar is equal to 50 micrometers.

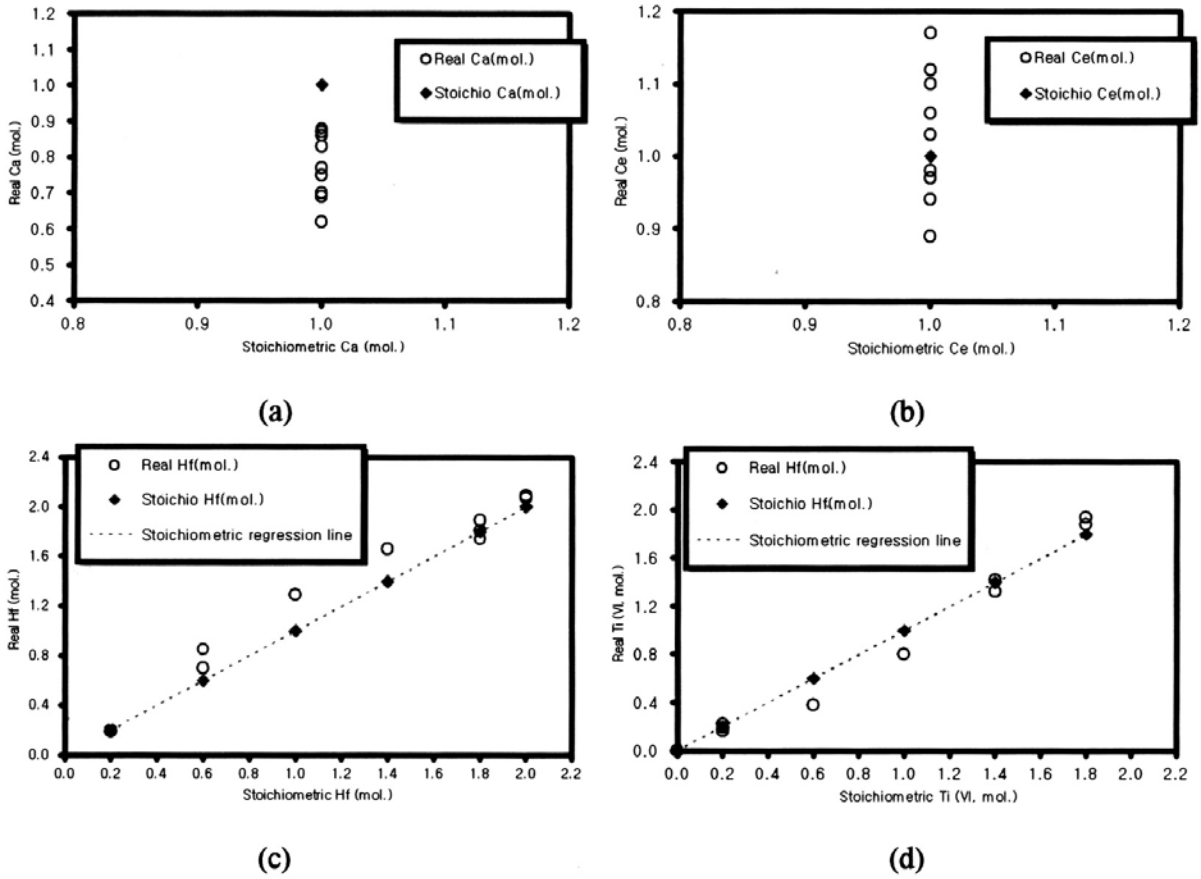

Fig. 4. Comparison between real and nominal stoichiometric compositions.

Discussion

Except for unreacted starting materials (in some runs), perovskite, pyrochlore and A_2BO_5 oxide were formed in the system of Ca-Ce-Hf-Ti-O. D-spacings (indicate the strongest diffraction intensity of phases in XRD diffraction patterns) of perovskite and pyrochlore increased with increasing the content of Hf (Table I). 2.71A-perovskite dominated up to x=1.4, and 2.83A-perovskite (perovskite-II) larger than x=1.4 (Table I). D-spacings of pyrochlores were 2.93A at x=0.2-0.6, 2.98A at x=1.0, and 3.02A at x=1.4-2.0. In addition to the variation of d-spacings in pyrochlores, their lattice constants also increased with the content of Hf (Table I and Table II).

Table II. Ionic Radii, Ratio and Lattice Constant of Pyrochlore Calculated for Nominal Stoichiometry ($CaCeHf_xTi_{2-x}O_7$: x=0.2-2.0) and Actual Chemical Compositions Analyzed by EDS.

Compositions	Ionic Radii (A)		Ratio	Lattice constant
	Ca and Ce (VIII)	Hf and Ti (VI)	VIII/VI	a (A)
Initial Batch Compositions				
X=0.2	1.045	0.616	1.6978	10.158
X=0.6	1.045	0.637	1.6418	10.236
X=1.0	1.045	0.658	1.5894	10.331
X=1.4	1.045	0.679	1.5402	10.415
X=1.8	1.045	0.700	1.4939	10.459
X=2.0	1.045	0.710	1.4718	10.473
Real Chemical Compositions analyzed by EDS				
X=0.2	1.042	0.615	1.6949	10.158
X=0.6	1.042	0.643	1.6198	10.236
X=1.0	1.033	0.670	1.5418	10.331
X=1.4	1.027	0.690	1.4884	10.415
X=1.8	1.029	0.700	1.4705	10.459
X=2.0	1.026	0.710	1.4451	10.473

Hence unit cell dimension is closely related with the ionic radii of elements, which occupy not only eight-coordinated site, but also six-coordinated site. Although Yamamura et al. [15] pointed out that ionic radii ratio was directly proportional to the lattice constant in pyrochlore, the relationship was reverse to our data (Table II). Such difference was from which Yamamura and coworkers treated only Zr-based pyrochlore. Namely, their direct proportional relationship can be applied only for occasion, which all the six-coordinated sites are occupied by the same element. Table III showed ionic radii ratios, phases and lattice constants of pyrochlores (refer to data of the JCPDS cards). Lattice constants (and ionic radii ratio) of $Sm_2Ti_2O_7$ and $Tb_2Ti_2O_7$ are a=10.23A (r^{VIII}/r^{VI}=1.783) and a=10.145A (r^{VIII}/r^{VI}=1.04), respectively. In these cases, ionic radii ratios are in direct proportion to the lattice constants as the relationship presented by Yamamura et al. [15]. However, the relationship of $Sm_2Sn_2O_7$ (a=10.508A; r^{VIII}/r^{VI}=1.564) and $Sm_2Zr_2O_7$ (a=10.590A; r^{VIII}/r^{VI}=1.499) was in inverse proportion like our results.

The stability of pyrochlore ($[A_2]^{VIII}[B_2]^{VI}O_7$) structure is governed by the ionic radii ratio of the $[A]^{VIII}$ and $[B]^{VI}$ site cations (r_A^{VIII}/r_B^{VI}). The range of pyrochlores stability extends from r_A^{VIII}/r_B^{VI}=1.46 for $Gd_2Zr_2O_7$ to r_A^{VIII}/r_B^{VI}=1.78 for $Sm_2Ti_2O_7$. For smaller ionic radii ratios (r_A^{VIII}/r_B^{VI}<1.46), anion-deficient fluorite is the stable structure, whereas the monoclinic structure is stable for ionic radii ratios r_A^{VIII}/r_B^{VI} >1.78 [8].

Ionic radii ratios (r_A^{VIII}/r_B^{VI}=1.47-1.70: Table II) of pyrochlore calculated from all stoichiometric compositions belonged to the stability range of pyrochlore structure. Also, the ionic radii ratios (r_A^{VIII}/r_B^{VI}=1.47-1.70), which were calculated from real compositions analyzed with EDS analyzer, similar to those calculated from batch compositions except at x=2.0 (r_A^{VIII}/r_B^{VI}=1.45).

Although the ratio at x=2.0 was below the stability range of pyrochlore structure, XRD data showed the existence of pyrochlore (Table I, and Fig. 2f). We inferred that such discrepancy due to the gap in establishment of the stability range of pyrochlore structure in previous studies or to the difference of the elements occupied six-coordinated site. Namely, $Lu_2Sn_2O_7$, stannates based oxide, has pyrochlore structure, although the ionic radii ratio is 1.42 (Table III).

Table III. Ionic Radii Ratios (r_A^{VIII}/r_B^{VI}), Phases and Lattice Constants (a) of Lanthanide Pyrochlores (From JCPDS card, 1993).

A^{VIII} \ B^{VI}		Ti(4+)			Sn(4+)			Hf(4+)			Zr(4+)		
		0.605A	Phase	a(A)	0.690A	Phase	a(A)	0.710A	Phase	a(A)	0.720A	Phase	a(A)
La	1.160	1.917	N/A		1.681	Pyro	10.702	1.634	F	5.382	1.611	Pyro	10.793
Ce	1.143	1.889	N/A		1.657	N/A		1.610	N/A		1.588	?	10.700
Pr	1.126	1.861	N/A		1.632	Pyro	10.604	1.586	?	10.690	1.564	Pyro	10.700
Nd	1.109	1.833	N/A		1.607	Pyro	10.573	1.562	F	5.316	1.540	Pyro	10.648
Pm	1.093	1.807	N/A		1.584	N/A		1.539	N/A		1.518	N/A	
Sm	1.079	1.783	Pyro	10.230	1.564	Pyro	10.508	1.520	F	5.287	1.499	Pyro	10.590
Eu	1.066	1.762	Pyro	10.193	1.545	Pyro	10.474	1.501	F	5.268	1.481	Pyro	10.531
Gd	1.053	1.740	Pyro	10.180	1.526	Pyro	10.460	1.483	F	5.258	1.463	?	10.501
Tb	1.040	1.719	Pyro	10.145	1.507	Pyro	10.428	1.465	N/A		1.444	N/A	
Dy	1.027	1.698	Pyro	10.106	1.488	Pyro	10.389	1.446	F	5.218	1.426	N/A	
Y	1.019	1.684	Pyro	10.091	1.477	Pyro	10.371	1.435	N/A		1.415	N/A	
Ho	1.015	1.678	Pyro	10.102	1.471	Pyro	10.374	1.430	F	5.206	1.410	?	10.380
Er	1.004	1.660	Pyro	10.076	1.455	Pyro	10.350	1.414	F	5.189	1.394	N/A	
Tm	0.994	1.643	Pyro	10.055	1.441	Pyro	10.330	1.400	F	5.168	1.381	N/A	
Yb	0.985	1.628	Pyro	10.030	1.428	Pyro	10.304	1.387	N/A		1.368	N/A	
Lu	0.977	1.615	Pyro	10.019	1.416	Pyro	10.294	1.376	N/A		1.357	N/A	

N/A: not available, Pyro: pyrochlore (Fd3m), F: fluorite (Fm3m), ?: Unknown (F).

CONCLUSIONS

The phases synthesized from various stoichiometric compositions ($CaCeHf_xTi_{2-x}O_7$: x=0.2-2.0) and conditions (1200°C-1600°C for 20 hr) were found to be perovskite, pyrochlore and A_2BO_5oxides. The optimum synthetic conditions of pyrochlores are as follows: 1300°C at x = 0.2, 1400°C at x = 0.6 and 1500°C at x = 1.0-2.0. Pyrochlore, however, was coexisted with minor CeO_2 or perovskite instead of the appearance of single phase even at these optimal conditions. It was due to the non-stoichiometric composition of pyrochlore. Pyrochlore and perovskite indicated the characteristics that their d-spacings and lattice constants increased with increasing the content of hafnium. It suggested that lattice constant be related to the ionic radii of elements, which occupy not only eight-coordinated sites, but also six-coordinated sites. Ionic radii ratio (r_A^{VIII}/r_B^{VI}=1.47-1.70) of pyrochlores belonged to the stability range of pyrochlore except for x=2.0 (r_A^{VIII}/r_B^{VI} =1.45). Because XRD data, however, showed the existence of pyrochlore, we inferred that such discrepancy due to the gap in the establishment of the stability range of pyrochlore structure in previous studies or to the difference of the elements occupied six-

coordinated sites.

REFERENCES

1. R. E. Williford, and W. J. Weber, "Computer simulation of Pu^{3+} and Pu^{4+} substitutions in gadolinium zirconate," J. Nucl. Mat., 299, 140-147 (2001).
2. A. E. Ringwood, "Disposal of high-level nuclear waste: a geological perspective," Mineralogical Magazine, Vol.49, Pt.2, 159-176 (1985).
3. A. E. Ringwood, S. E. Kesson, K. D. Reeve, J. L. Woolfrey, and E. J. Ramm, "Radioactive waste forms for the future, edited by W. Lutze and Ewing, R.C.," Elsev., Amst., 233 (1988).
4. E. R. Vance, B. D. Begg, R. A. Day, C. J. Ball, "Zirconolite-rich ceramics for actinide wastes," In: Scientific Basis for Nuclear Waste Management-XVIII. MRS Symposia Proceedings, Vol.353, Pt.2, 767-774 (1995).
5. S. Luo, X. Zhu, and B. Tang, "Actinides containment by using zirconolite-rich Synroc," In: Proceedings of International Meeting on Nuclear and Hazardous Waste Management (Spectrum 98), American Nuclear Society, La Grange Park, IL, 829-833 (1998).
6. N. K. Kulkarni, S. Sampath, and V. Venugopal, "Preparation and characterization of Pu-pyrochlore: $[La_{1-x}Pu_x]_2Zr_2O_7$ (x=0-1)," J. Nucl. Mater., 281, 248-250 (2000).
7. A. J. Feighery, J. T. S. Irvine, and S. Zheng, "Phase relation at 1500 in the ternary system ZrO_2-Gd_2O_3-TiO_2," J. Solid State Chemistry, 160, 302-306 (2001).
8. B. D. Begg, N. J. Hess, D. E. McCready, S. Thevuthasan, and W. J. Weber, "Heavy-ion irradiation effects in $Gd_2(Ti_{2-x}Zr_x)O_7$ pyrochlore," J. Nucl. Mat., 289, 188-193 (2001).
9. B. D. Begg, N. J. Hess, W. J. Weber, R. Devanathan, J. P. Icenhower, S. Thevuthasan, and B. P. McGrail, "Heavy-ion irradiation effects on structures and acid dissolution of pyrochlore," J. Nucl. Mat., 228, 208-216 (2001).
10. N. P. Laverov, S. V. Yudintsev, S. V. Stefanovsky, and Y. N. Jang, "New actinide matrix with pyrochlore structure," Doklady of the Russian Academy of Sciences, 381A, 9, 1053-1056 (2001).
11. N. P. Laverov, S. V. Yudintsev, S. V. Stefanovsky, Y. N. Jang, M. I. Lapina, A. V. Sivtsov, and R. C. Ewing, "Phase transformations during synthesis of actinide matrices," Doklady of the Russian Academy of Sciences, 385A, 6, 671-675 (2002).
12. P. E. Raison, R. G. Haire, T. Sato, and T. Ogawa, "Fundamental and technological aspects of actinide oxide pyrochlores: Relevance for immobilization matrices," In: Scientific Basis for Nuclear Waste Management-XXII. MRS Symposium Proceedings, 556, 3-10 (1998).
13. R. Schrempf, "New Rad-Resistant material for safer plutonium storage," Energy Science

News April (http://www.jlab.org/news/internet/2000/rad_resistant.html) (2000).

14. Yu. A. Teterin, S. V. Stefanovskii, S. V. Yudintsev, G. N. Bek-Uzarov, A. Yu. Tetrerin, K. I. Maslakov, and I. O. Utkin, "X-ray photoelectron study of calcium cerium titanate ceramics," Russian Journal of Inorganic Chemistry, 49, 1, 87-94 (2004).
15. H. Yamamura, H. Nishino, K. Kakinuma, K. Nomura, "Electrical conductivity anomaly around fluorite-pyrochlore phase boundary," Solid State Ionics, 158, 359-365 (2003).